Hydrol. Earth Syst. Sci., 14, 925–940, 2010
www.hydrol-earth-syst-sci.net/14/925/2010/
doi:10.5194/hess-14-925-2010

Hydrology and Earth System Sciences

Simulation of snow accumulation and melt in needleleaf forest environments

C. R. Ellis, J. W. Pomeroy, T. Brown, and J. MacDonald

Centre for Hydrology, University of Saskatchewan, 117 Science Place, Saskatoon, Saskatchewan, S7N 5C8, Canada

Received: 15 January 2010 – Published in Hydrol. Earth Syst. Sci. Discuss.: 9 February 2010
Revised: 5 May 2010 – Accepted: 7 May 2010 – Published: 14 June 2010

Abstract. Drawing upon numerous field studies and modelling exercises of snow processes, the Cold Regions Hydrological Model (CRHM) was developed to simulate the four season hydrological cycle in cold regions. CRHM includes modules describing radiative, turbulent and conductive energy exchanges to snow in open and forest environments, as well as account for losses from canopy snow sublimation and rain evaporation. Due to the physical-basis and rigorous testing of each module, there is a minimal need for model calibration. To evaluate CRHM, simulations of snow accumulation and melt were compared to observations collected at paired forest and clearing sites of varying latitude, elevation, forest cover density, and climate. Overall, results show that CRHM is capable of characterising the variation in snow accumulation between forest and clearing sites, achieving a model efficiency of 0.51 for simulations at individual sites. Simulations of canopy sublimation losses slightly overestimated observed losses from a weighed cut tree, having a model efficiency of 0.41 for daily losses. Good model performance was demonstrated in simulating energy fluxes to snow at the clearings, but results were degraded from this under forest cover due to errors in simulating sub-canopy net longwave radiation. However, expressed as cumulative energy to snow over the winter, simulated values were 96% and 98% of that observed at the forest and clearing sites, respectively. Overall, the good representation of the substantial variations in mass and energy between forest and clearing sites suggests that CRHM may be useful as an analytical or predictive tool for snow processes in needleleaf forest environments.

Correspondence to: C. R. Ellis
(cre152@mail.usask.ca)

1 Introduction

Needleleaf forests dominate much of the mountain and boreal regions of the northern hemisphere where snowmelt is the most important hydrological event of the year (Gray and Male, 1981). The retention of foliage by evergreen needleleaf tree species during winter acts to decrease snow accumulation via canopy interception losses (Schmidt, 1991; Lundberg and Halldin, 1994; Pomeroy et al., 1998a) and greatly modify energy exchanges to snow (Link and Marks, 1999; Gryning and Batchvarova, 2001; Ellis et al., 2010). However, forest cover is often discontinuous, containing clearings of varying dimensions which may differ considerably in snow accumulation (McNay, 1988) and melt characteristics (Metcalfe and Buttle, 1995). As such, management of water derived from forest snowmelt is expected to benefit from the effective prediction of snow accumulation and melt in both forest and open environments.

Forest cover varies in its effects upon snow accumulation, with reductions of 30% to 50% of that in nearby clearings observed in cold Canadian and Russian mountain and boreal forests (Pomeroy and Gray, 1995; Pomeroy et al., 2002; Gelfan et al., 2004) to nearly even accumulations reported in temperate Finnish forests (Koivusalo and Kokkonen, 2002). Although numerous mechanisms have been proposed to explain decreased snow accumulations in forests, sublimation of canopy snow has been shown to be the primary factor controlling forest snow losses (Troendle and King, 1985; Schmidt et al., 1988; Pomeroy and Schmidt, 1993; Lundberg and Halldin, 1994; Parviainen and Pomeroy, 2000). Investigations by Pomeroy and Gray (1995) and Pomeroy et al. (1998a) found that 30 to 45% of annual snowfall in western Canada may be lost by canopy sublimation due to the increased exposure of intercepted snow to the above atmosphere. Thus, the estimation of canopy sublimation losses

Published by Copernicus Publications on behalf of the European Geosciences Union.

have often made appeal to physically-based "ice-sphere" models (e.g. Schmidt, 1991) which adjust sublimation losses from a single, small ice-sphere for the decreased exposure of canopy snow to the atmosphere. Such methods have been shown to well approximate canopy sublimation losses over multiple snowfall events through the coupling of the multi-scale sublimation model to a needleleaf forest interception model (Pomeroy et al., 1998a).

Alongside interception effects, needleleaf forest cover also influences energy exchanges to snow. The forest layer acts to effectively decouple the above-canopy and sub-canopy atmospheres, resulting in a large suppression of turbulent energy fluxes (Harding and Pomeroy, 1996; Link and Marks, 1999). Consequently, energy to sub-canopy snow is dominated by radiation; itself modified by the canopy through the shading of shortwave irradiance while increasing longwave irradiance from canopy thermal emissions (Link et al., 2004; Sicart et al., 2004; Pomeroy et al., 2009). Forest cover may also affect sub-canopy shortwave radiation by altering snow surface albedo through deposition of forest litter on snow (Hardy et al., 2000; Melloh et al., 2002), or by influencing energy-controlled snow metamorphism rates (Ellis et al., 2010). As such, simulations of forest effects on energy to snow have largely focused on the adjustment of shortwave and longwave fluxes (Hardy et al., 2004; Essery et al., 2008; Pomeroy et al., 2009), although methods estimating turbulent energy transfer in forests have also been described (Hellström, 2000; Gelfan et al., 2004).

Since the first successful demonstration of snowmelt simulation using an energy-balance approach by Anderson (1976), numerous such snowmelt models have developed (e.g. EBSM, Gray and Landine, 1988; SNTHERM, Jordan, 1991; SHAW, Flerchinger and Saxton, 1989; Snobal, Marks et al., 1999). Due to the differing objective specific to each model, there is considerable variation in the detail to which snow energetics may be described, as well as forcing data and parameterization requirements. In general, more sophisticated snowmelt models possess information requirements that may prohibit their successful employment in more remote environments, where forcing data and parameter information is typically lacking or poorly approximated. Instead, more basic models that maintain a physically-based representation of forest snow processes in cold regions are expected to be better suited for such environments.

Although much focus has been placed on simulating forest snow accumulation and melt processes separately, fewer simulations over the entire snow accumulation and melt period have been demonstrated. To this end, this paper outlines and evaluates the simulation of snow accumulation and melt in paired forest and clearing sites of varying forest cover density and climate using the Cold Regions Hydrological Model (CRHM). CRHM is a deterministic model of the hydrological cycle containing process algorithms (modules) developed from field investigations in cold region environments, with modest data and parameter requirements. This paper examines the potential for CRHM to be used to analyze and predict how changes in climate and forest-cover may affect snow processes in cold region forests.

2 Model description

Described in detail by Pomeroy et al. (2007), CRHM operates through interaction of its four main components: (1) observations, (2) parameters, (3) modules, and (4) variables and states. The description of each component below focuses on the requirements of CRHM for forest environments:

1. Observations: CRHM requires the following meteorological forcing data for each simulation timestep, t (units in [ ]):
   a air temperature , T_a [°C];
   b humidity, either as vapour pressure, e_a [kPa] or relative humidity, RH [%];
   c precipitation, P [kg m^{-2}];
   d wind speed, observed either above, or within the canopy, u [m s^{-1}];
   e shortwave irradiance, $K\downarrow$ [W m^{-2}] (in the absence of observations, $K\downarrow$ may be estimated from T_a);
   f longwave irradiance, $L\downarrow$ [W m^{-2}] (in the absence of observations, $L\downarrow$ may be estimated from T_a and e_a).
2. Parameters: provides a physical description of the site, including latitude, slope and aspect, forest cover density, height, species, and soil properties. In CRHM, forest cover need only be quantified by an effective leaf area index (LAI') and forest height (h); the forest sky view factor (v) may be specified explicitly or estimated from LAI'. The heights at which meteorological forcing data observations are collected are also specified here.
3. Modules: algorithms implementing the particular hydrological processes are selected here by the user.
4. Initial states and variables: specified within the appropriate module.

3 Modules

The following provides a general outline of the main modules and associated algorithms in CRHM.

3.1 Observation module

To allow for the distribution of meteorological observations away from the point of collection, appropriate corrections are applied to observations within the *observation* module. These include the correction of air temperature, humidity,

and the amount and phase of precipitation for elevation, as well as correction of shortwave and longwave irradiance for topography.

3.2 Snow mass-balance module

In CRHM, snow is conserved within a single defined spatial unit, with changes in mass occurring only through a divergence of incoming and outgoing fluxes. In clearing environments, snow water equivalent (SWE) [kg m^{-2}] at the ground may be expressed by the following mass-balance of vertical and horizontal snow gains and losses

$$\mathrm{SWE} = \mathrm{SWE}_o + (P_s + P_r + H_{\mathrm{in}} - H_{\mathrm{out}} - S - M)t \quad (1)$$

where t is the time step in the model calculation, SWE_o is the antecedent snow water equivalent [kg m^{-2}], P_s and P_r are the respective snowfall and rainfall rates, H_{in} is the incoming horizontal snow transport rate, H_{out} is the outgoing horizontal snow transport rate, S is the sublimation loss rate, and M is the melt loss rate [all units kg m$^{-2}t^{-1}$]. In forest environments Eq. (1) is modified to

$$\mathrm{SWE} = \mathrm{SWE}_o + (P_s - (I_s - U_l) + P_r - (I_r - R_d) - M)t \quad (2)$$

in which I_s is canopy snowfall interception rate, U_l is the rate of canopy snow unloading, I_r is the canopy rainfall interception rate, and R_d is the rate of canopy rain drip [all units kg m$^{-2}t^{-1}$].

The amount of snowfall intercepted by the canopy is dependent on various physical factors, including tree species, forest density, and the antecedent intercepted snowload ($I_{s,o}$) [kg m^{-2}]. In CRHM, a dynamic canopy snow-balance is calculated, in which the amount of snow interception (I_s) is determined by

$$I_s = (I_s^* - I_{s,o})(1 - e^{-C_l P_s t / I_s^*}) \quad (3)$$

where C_l is the "canopy-leaf contact area" per unit ground [], and I^*_s is the species-specific maximum intercepted snowload [kg m^{-2}], which is determined as a function of the mean maximum snowload per unit area of branch, $\overline{S}$ [kg m^{-2}], the density of falling snow, ρ_s [kg m^{-3}], and LAI$'$ by

$$I_s^* = \overline{S}\left(0.27 + \frac{46}{\rho_s}\right)\mathrm{LAI}'. \quad (4)$$

Sublimation of intercepted snow is estimated following the Pomeroy et al. (1998) multi-scale model, in which the sublimation rate coefficient for intercepted snow, V_i [s^{-1}], is multiplied by the intercepted snowload to give the canopy sublimation flux, q_e [kg m^{-2} s^{-1}], i.e.

$$q_e = V_i\, I_s. \quad (5)$$

Here, V_i is determined by adjusting the sublimation flux for a 500 µm radius ice-sphere, V_s [s^{-1}], by the intercepted snow exposure coefficient, C_e [], i.e.

$$V_i = V_s\, C_e, \quad (6)$$

in which C_e is defined by Pomeroy and Schmidt (1993) as

$$C_e = k\left(\frac{I_s}{I*_s}\right)^{-F}. \quad (7)$$

where k is a dimensionless coefficient indexing the shape of intercepted snow (i.e. age and structure) and F is an exponent value of approximately 0.4. The ventilation wind speed of intercepted snow may be set as an observed within-canopy wind speed, or approximated from above-canopy wind speed by

$$u_\xi = u_h\, e^{-\psi\xi} \quad (8)$$

where u_ξ [m s^{-1}] is the estimated within-canopy wind speed at a fraction ξ of the entire forest depth [], u_h is the wind speed at the canopy top [m s^{-1}], and ψ is the canopy wind speed extinction coefficient [], which is determined as a linear function of LAI' for various needleleaf species (Eagleson, 2002). Unloading of intercepted snow to the sub-canopy snowpack is calculated as an exponential function of time following Hedstrom and Pomeroy (1998). Additional unloading resulting from melting intercepted snow is estimated by specifying a threshold ice-bulb temperature (T_b) in which all intercepted snow is unloaded when exceeded for three hours (Gelfan et al., 2004).

3.3 Rainfall interception and evaporation module

Although the overall focus of this manuscript is that of snow-forest interactions, winter rainfall may represent substantial water and energy inputs to snow. The fraction of rainfall to sub-canopy snow received as direct throughfall is assumed to be inversely proportional to the fractional horizontal canopy coverage (C_c) []. All other rainfall is intercepted by the canopy, which may be lost via evaporation (E) [kg m$^{-2}t^{-1}$] or dripped to the sub-canopy if the canopy rain storage (C_R) [mm] exceeds the maximum canopy storage ($S_{\max}$) [mm]. Here, direct throughfall and drip to the sub-canopy are added to the water equivalent of the snowpack. The intercepted rainload ($I_{r,o}$) [kg m^{-2}] in CRHM is estimated using a simplified Rutter model approach (Rutter, 1971) in which a single storage is determined and scaled for sparse canopies by C_c (e.g. Valente et al., 1997). Evaporation from a fully-wetted canopy (E_p) [kg m$^{-2}t^{-1}$] is calculated using the Penman-Monteith combination equation (Monteith, 1965) for the case of no stomatal resistance, i.e.

$$\mathrm{E} = C_c E_p \qquad \text{for } C_R = S_{\max}. \quad (9)$$

For partially-wetted canopies E is reduced in proportion to the degree of canopy saturation, i.e.

$$\mathrm{E} = C_c E_p C_{\mathrm{R}}/S_{\max} \qquad \text{for } C_R < S_{\max}. \quad (10)$$

3.4 Snow energy-balance module

Energy to snow ($Q*$) is resolved in CRHM as the sum of radiative, turbulent, advective and conductive energy fluxes to snow, i.e.

$$K*+L*+Q_h+Q_e+Q_g+Q_p=\frac{dU}{dt}+Q_m=Q* \quad (11)$$

where Q_m is the energy for snowmelt, $\mathrm{d}U/\mathrm{d}t$ is the change in internal (stored) energy of snow, $K*$ and $L*$ are net shortwave and longwave radiations, respectively, Q_h and Q_e are the net sensible and latent heat turbulent fluxes, respectively, Q_g is the net ground heat flux, and Q_p is the energy from rainfall advection [all units $\mathrm{MJ\,m^{-2}}t^{-1}$]. In Eq. (11), positive magnitudes represent energy gains to snow and negative magnitudes are energy losses. The amount of melt (M) is calculated from Q_m by

$$M=\frac{Q_m}{\rho_w B\,\lambda_f} \quad (12)$$

where ρ_w is the density of water [$\mathrm{kg\,m^{-3}}$], B is the fraction of ice in wet snow [$\sim$0.95−0.97], and λ_f is the latent heat of fusion for ice [$\mathrm{MJ\,kg^{-1}}$].

3.4.1 Adjustment of energy fluxes to snow for needleleaf forest cover

For the purpose of brevity, the following section outlines the algorithms in CRHM estimating energy fluxes in forest environments only. For an overview of energy flux estimations by CRHM in open environments, refer to Pomeroy et al. (2007).

Shortwave radiation to forest snow

In CRHM, net shortwave radiation to forest snow ($K*_f$) is equal to the above-canopy irradiance ($K\downarrow$) transmitted through the canopy less the amount reflected from snow, expressed here as

$$K*_f=K\downarrow\tau(1-\alpha_s) \quad (13)$$

in which α_s is the snow surface albedo [], the decay of which is approximated as a function of time subsequent to a snowfall event, and τ is the forest shortwave transmittance [], which is estimated by the following variation of Pomeroy and Dion's (1996) formulation (Pomeroy et al., 2009)

$$\tau=e^{-\frac{1.081\theta\cos(\theta)\mathrm{LAI}`}{\sin(\theta)}} \quad (14)$$

where θ is the solar angle above the horizon [radians].

Longwave radiation to forest snow

As stated previously, longwave irradiance to forest snow ($L\downarrow_f$) may be enhanced relative to that in the open as the result of thermal emissions from the canopy. Simulation of $L\downarrow_f$ is made as the sum of sky and forest longwave emissions weighted by the sky view factor (v), i.e.

$$L\downarrow_f=vL\downarrow+(1-v)\varepsilon_f\sigma T_f^4. \quad (15)$$

Here, ε_f is the forest thermal emissivity [], σ is the Stefan-Boltzmann constant [$\mathrm{W\,m^{-2}\,K^{-4}}$], and T_f is the forest temperature [K]. Longwave exitance from snow ($L\uparrow$) is determined by

$$L\uparrow=\varepsilon_s\sigma T_s^4 \quad (16)$$

where ε_s is the thermal emissivity of snow [], and T_s is the snow surface temperature [K] which is resolved using the longwave psychrometric formulation by Pomeroy and Essery (2010):

$$T_s=T_a+\frac{\varepsilon_s\left(L\downarrow-\sigma T_a^4\right)+\lambda_s(w_a-w_s)\rho_a/r_a}{4\varepsilon_s\sigma T_a^3+(c_p+\lambda_s\Delta)\rho_a/r_a} \quad (17)$$

where w_a and w_s are the specific and saturation mixing ratios [], ρ_a is the air density [$\mathrm{kg\,m^{-3}}$], c_p is the specific heat capacity of air [$\mathrm{J\,kg^{-1}K^{-1}}$], λ_s is the latent heat of sublimation [$\mathrm{MJ\,kg^{-1}}$], r_a is the aerodynamic resistance [$\mathrm{s\,m^{-1}}$], and Δ is the slope of the saturation vapour pressure curve [$\mathrm{kPa\,K^{-1}}$].

Sensible (Q_h) and latent (Q_e) heat fluxes

Determination of Q_h and Q_e in open and forest sites are made using the following semi-empirical formulations developed by Gray and Landine (1988):

$$Q_h=\text{-}0.92+0.076u_{\mathrm{mean}}+0.19T_{\max} \quad (18)$$

$$Q_e=0.08(0.18+0.098u_{\mathrm{mean}})\ (6.11-10ea_{\mathrm{mean}}) \quad (19)$$

where u_{mean} is the mean daily wind speed [$\mathrm{m\,s^{-1}}$], $T_{\max}$ is the maximum daily air temperature [°C], and ea_{mean} is the mean daily vapour pressure [kPa]. For the case of rainfall to melting snow (i.e. T_s=0°C), the energy delivered to the snowpack via rainfall advection (Q_p) is given by

$$Q_p=4.2\times10^{-3}(P_r-I_r)T_r \quad (20)$$

where T_r is the rainfall temperature [°C], which is approximated by T_a. The primary mass and energy balance calculation routines for both forest and clearing environments within CRHM are summarized in Fig. 1.

4 Model application

Simulations of snow accumulation and melt using CRHM were performed at five paired forest and clearing sites of varying location, climate, forest species, and forest cover density (Table 1). With the exception of the Marmot Creek sites, all simulations were performed as part of the second

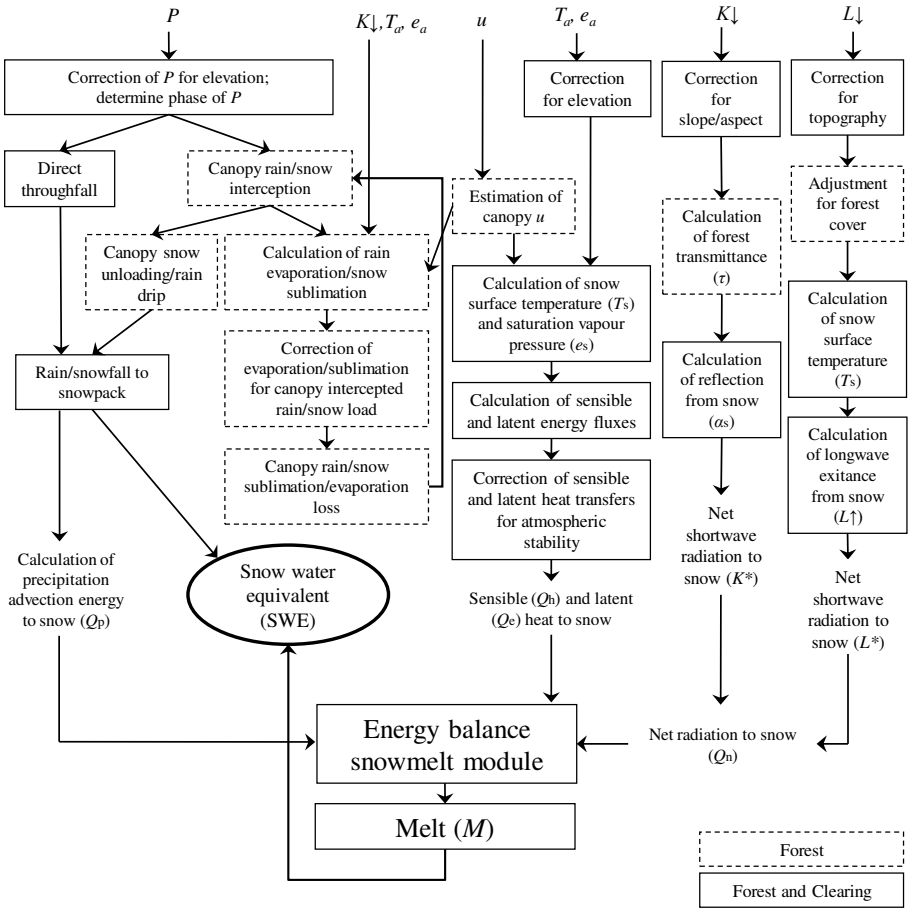

Fig. 1. Schematic outlining the major mass and energy calculations involved in the forest component of the Cold Regions Hydrological Model (CRHM).

snow model inter-comparison project (SnoMIP2) (Rutter et al., 2009; Essery et al., 2009). This initiative involved the off-line simulation of snow accumulation and melt in paired forest and nearby clearing sites located in Canada, Switzerland, Finland, Japan and the United States. Hourly standard meteorological forcing data, site descriptions, and initial states were provided to each participant by the SnoMIP2 facilitators. All simulations in SnowMIP2 were executed "blindly" with the exception of the Switzerland location for the 2002–2003 season where SWE field data were provided to allow for the option of model calibration. Location, topography and forest cover descriptions for all sites are given in Table 1, and site pictures in Fig. 2. Simulations of snow accumulation and melt were performed for both forest and adjacent forest clearing sites at each location for the period extending from 1 October to approximately 1 June. For each simulation timestep, appropriate energy, mass, and state variables were outputted by the model.

4.1 Simulation of snow accumulation and melt

4.1.1 Evaluation of model performance

Simulations of snow accumulation and melt by CRHM were evaluated in terms of the ability of representing:

1. the variation in mean and maximum seasonal SWE observed between all sites; and

2. the timing and quantity of SWE accumulation and melt at individual sites.

For 1 and 2 above, model performance was assessed by the following three measures: the model bias index (MB), the model efficiency index (ME), and the root mean square error (RMSE). These indexes were used as they provide a rather complementary evaluation of model performance, with the MB comparing the total simulation output to the total of observations, the ME an indication of model performance compared to the mean of the observations, and the RMSE a

Alptal, Switzerland forest (left) and clearing (right).

BERMS, Saskatchewan, Canada forest (left) and clearing (right).

Fraser, Colorado, USA forest (left) and clearing (right).

Marmot Creek, Alberta, Canada pine forest (left) and clearing (right).

Marmot Creek, Alberta, Canada spruce forest showing the suspended spruce tree (left), the spruce clearing (centre) and reference radiation tower at the spruce clearing (right).

Fig. 2. Photographs of meteorological stations located at forest and clearing sites at Alptal, Switzerland; BERMS, Saskatchewan, Canada; Fraser, Colorado, USA; and pine and spruce sites at Marmot Creek, Alberta, Canada (with the exception of the Marmot Creek sites, site photographs were provided by the SnowMIP2 facilitators).

Table 1. Location, topography, and forest cover descriptions of paired clearing and forest sites used in simulations of snow accumulation and melt.

Site:	Years	Latitude	Elevation aspect	Slope, species	Height,	LAI'	v
Alptal, Switzerland (forest)	2002–2004	47°3′ N	1185 m	3° W	25 m spruce and fir	2.5	0.04
Alptal, Switzerland (clearing)	2002–2004	47°3′ N	1220 m	11° W	–	–	–
BERMS, Saskatchewan, Canada (forest)	2002–2003	53°55′ N	579 m	level	12–15 m jack pine	1.66	0.28
BERMS, Saskatchewan, Canada (clearing)	2002–2003	53°57′ N	579 m	level	–	–	–
Fraser, Colorado, USA (forest)	2003–2005	39°53′ N	2820 m	17°, 305°	∼ 27 m pine, spruce/fir	3	not given
Fraser, Colorado, USA (clearing)	2003–2005	39°53′ N	2820 m	17°, 305°	2–4 m sparse trees	0.4	not given
Marmot Creek, Alberta, Canada (pine forest)	2007–2008	50°56′ N	1500 m	level	∼ 15 m lodgepole pine	1.5	0.20
Marmot Creek, Alberta, Canada (pine clearing)	2007–2008	50°56′ N	1430 m	level	–	–	–
Marmot Creek, Alberta, Canada (spruce forest)	2007–2008	50°56′ N	1850 m	level	17–20 m Engelmann spruce	2.0	0.15
Marmot Creek, Alberta, Canada (spruce clearing)	2007–2008	50°56′ N	1850 m	level	–	–	–

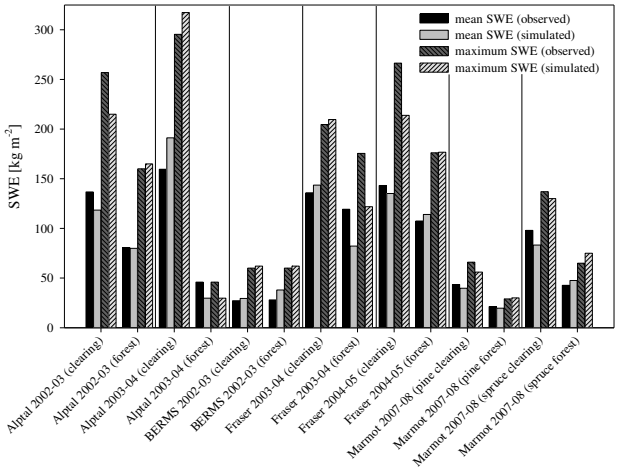

Fig. 3. Observed and simulated mean and maximum snow water equivalent (SWE) accumulations at forest and clearing sites.

quantification of the absolute unit error between simulations and observations. Here, the MB is calculated as

$$\mathrm{MB} = \frac{\sum_{i=1}^{n} x_{\mathrm{sim}}}{\sum_{i=1}^{n} x_{\mathrm{obs}}} \tag{21}$$

where x_{sim} and x_{obs} are the respective simulated and observed values at a given timestep for n number of paired simulated and observed values. Accordingly, MB values less than 1 signify an overall under-prediction by the model, and values greater than 1 an overall over-prediction by the model. The model efficiency index (ME) is given by

$$\mathrm{ME} = 1 - \left[\frac{\sum_{i=1}^{n} (x_{\mathrm{sim}} - x_{\mathrm{obs}})^2}{\sum_{i=1}^{n} (x_{\mathrm{obs}} - x_{\mathrm{avg}})^2} \right] \tag{22}$$

where x_{avg} is the mean value of n number of x_{obs} values. In Eq. (22), model efficiency increases as the ME index approaches 1, which represents a perfect match between simulations and observations; 0 indicates an equal efficiency between simulations and the x_{avg}, with increasingly negative values signifying a progressively superior estimation by the x_{avg}. The root mean square error (RMSE) is determined by

$$\mathrm{RMSE} = \sqrt{\frac{1}{n} \sum_{i=1}^{n} (x_{\mathrm{sim}} - x_{\mathrm{obs}})^2} \tag{23}$$

Table 2. Model bias index (MB), model efficiency index (ME), and root mean square error (RMSE) of simulated mean and maximum snow water equivalent (SWE) at clearing sites, forest sites, and all sites.

	Mean SWE			Maximum SWE		
	Clearing	Forest	All	Clearing	Forest	All
Model bias (MB)	0.99	0.94	0.97	0.94	0.94	0.94
Model efficiency (ME)	0.97	0.93	0.96	0.92	0.87	0.90
Root mean square error (RMSE) [kg m^{-2}]	16.0	16.1	16.0	27.0	21.6	24.4

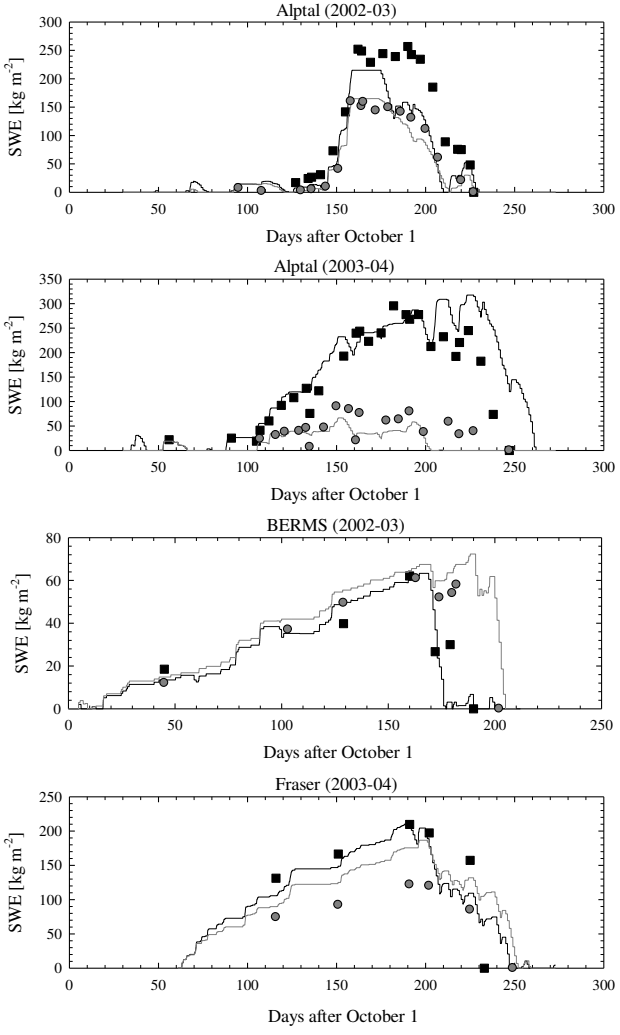

Fig. 4. Time series of observed and simulated SWE at paired forest and clearing sites.

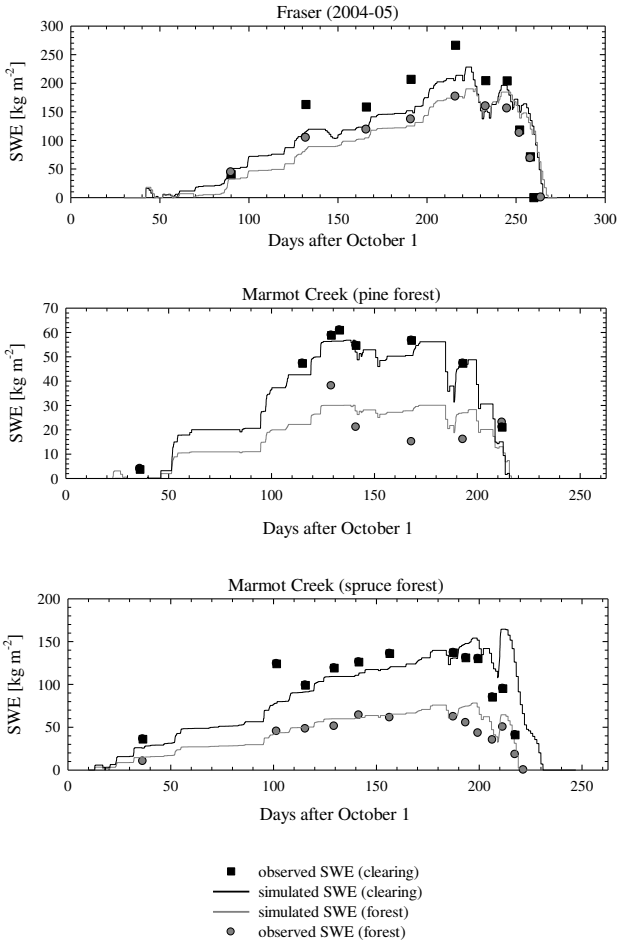

Fig. 4. Continued.

Simulation of mean and maximum winter SWE at all sites

Among all sites, considerable variation in mean and maximum seasonal SWE was observed, with mean SWE ranging from 20 to 160 kg m^{-2}, and maximum SWE from 29 to 295 kg m^{-2}. Large variations in SWE were also observed between paired forest and clearings, with forest accumulations ranging from approximately 30% of the clearing accumulation at the Alptal location (2003–2004) to near even accumulations at the BERMS location.

Simulated and observed mean and maximum SWE at all sites are shown in Fig. 3 with model performance index values given in Table 2. Here, simulations exhibit a small systematic under-prediction of mean SWE for all sites (MB=0.97), with a slightly greater under-prediction for the

Table 3. Determined model bias index (MB), model efficiency index (ME), and root mean square error (RMSE) for simulations of snow water equivalent (SWE) at individual sites.

Site:	MB []	ME []	RMSE [kg SWE m^{-2}]
Alptal 2002–2003 (clearing)	0.87	0.88	35.6
Alptal 2002–2003 (forest)	0.99	0.93	17.6
Alptal 2003–2004 (clearing)	1.20	0.64	51.1
Alptal 2003–2004 (forest)	0.65	−0.03	25.9
BERMS 2002–2003 (clearing)	1.14	0.70	12.6
BERMS 2002–2003 (forest)	1.12	0.63	12.9
Fraser 2003–2004 (clearing)	1.10	0.32	37.8
Fraser 2003–2004 (forest)	0.70	0.45	40.3
Fraser 2004-2005 (clearing)	0.95	0.32	37.8
Fraser 2004-05 (forest)	1.05	0.45	40.3
Marmot 2007-08 (pine clearing)	0.90	0.43	13.0
Marmot 2007–2008 (pine forest)	0.95	0.13	9.50
Marmot 2007–208 (spruce clearing)	0.80	0.58	28.0
Marmot 2007–2008 (spruce forest)	1.10	0.70	8.80
Clearing sites (mean)	0.99	0.55	30.8
Forest sites (mean)	0.94	0.47	22.2
All sites (mean)	0.97	0.51	26.5

forest sites. In comparison, a greater under-prediction of maximum SWE at all sites was realised (MB=0.94). Yet, the high ME value indicates CRHM well represented the variability in mean and maximum SWE accumulations between sites. Similar to MB results, the ME shows superior prediction of mean SWE to that of maximum SWE, as well as better prediction for clearing sites relative to forest sites. However, due to less snow at the forest sites, the lower MB and ME indexes at the forest sites translate into similar magnitudes of absolute error to that at the clearings (i.e. RMSE=$\sim$16 kg m^{-2}), and even lower absolute errors for the prediction of maximum SWE.

Simulation of winter SWE accumulation and melt at individual sites

Simulations of snow accumulation and melt at individual sites exhibited considerable variation in the accuracy of predicting the quantity and timing of SWE. However, as seen in Fig. 4, model simulations are able to capture the general differences in the timing of accumulation and melt between paired forest clearing sites. Model performance indexes for simulations at individual sites, as well as the mean index values for forest, clearing, and all sites are given in Table 3. Here, only small systematic underestimations of SWE are realised at both forest and clearing sites, having corresponding MB values of 0.94 and 0.99. In all, the mean ME for SWE simulations at individual sites was 0.51, with slightly lower efficiencies at the forest sites. Among simulations, the highest and lowest ME were both obtained at the Alptal forest site, with ME values of 0.93 and −0.03 for the 2002–2003 and 2003–2004 winters, respectively. Overall, the mean RMSE for all sites was 26.5 kg m^{-2}, with higher absolute errors for simulations at the clearing sites.

Due to the discontinuity of SWE observations over the winter at each site, exact determinations of the start, peak, and end of seasonal snow accumulation were not possible. Alternatively, an evaluation of the timing of snow accumulation was provided by the determination of the MB, ME, and RMSE of simulated SWE at the first, last and maximum SWE observation at each site (Table 4). Here, results show for the first observation, SWE is slightly over-predicted at the clearing sites (MB=1.07), with a large under-prediction of forest SWE (MB=0.6). At maximum SWE, little systematic simulation bias occurs for SWE simulations at all sites (MB=0.99) due to the offsetting of the slight over-prediction and under-prediction at the clearing and forest sites, respectively. However, for the last observed SWE, the high MB values indicate a large over-estimation of SWE at the end of melt, suggesting a substantial lag in simulated snow depletion. Poor simulation of late-season SWE is also reflected in the low ME and high RMSE as compared to results for the first and maximum SWE observations.

4.2 Simulation of canopy snow sublimation

The above results show CRHM is generally able to represent the observed differences in snow accumulation between paired forest and clearing sites. Considering that these differences are largely the result of canopy sublimation losses, model performance in estimating canopy sublimation

Table 4. Model bias index (MB), model efficiency index (ME) and root mean square error (RMSE) for simulations of SWE at the first SWE observation, maximum SWE observation, and last SWE observation at clearing sites, forest sites, and all sites.

	SWE at first observation			At maximum observed SWE			SWE at last observation		
	Clearing	Forest	All	Clearing	Forest	All	Clearing	Forest	All
MB []	1.07	0.60	0.89	1.08	0.95	0.99	3.85	3.59	3.64
ME []	0.96	0.91	0.93	0.87	0.89	0.88	−3.50	−5.97	−5.70
RMSE [kg SWE m^{-2}]	12.4	5.8	9.8	30.9	22.6	27.0	66.4	18.9	48.8

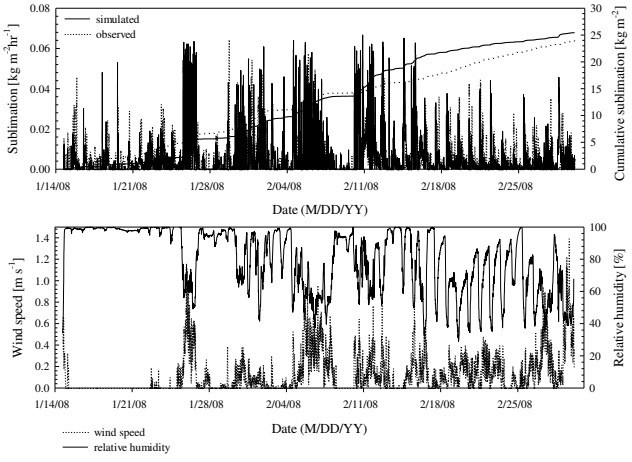

Fig. 5. Top: observed and simulated hourly (and cumulative) canopy snow sublimation; bottom: corresponding observations of forest wind speed and relative humidity.

is further investigated here. Evaluation of canopy sublimation was performed using canopy snowload measurements from a spruce tree suspended from a load cell at the Marmot Creek spruce forest site (Fig. 2). Changing tree weight was correlated to the intercepted snowload by the measured difference in snow accumulations between the forest and an adjacent clearing site (e.g. Hedstrom and Pomeroy, 1998). Decreases in tree tare from desiccation and needleleaf loss were accounted for, as was snow unloading from the canopy by measurements of snow collected in three lysimeters suspended under the canopy. Simulation of canopy sublimation was performed for the period of 14 January to 3 March using precipitation and incoming radiation data from the adjacent clearing with observations of within-canopy wind speed and humidity at the suspended tree.

Over the period, approximately one-half of snowfall was lost by canopy sublimation, with respective mean daily observed and simulated losses of 0.52 kg m^{-2} and 0.55 kg m^{-2}, giving a MB of 1.06 and a ME of 0.41. The time-series of hourly canopy sublimation losses in Fig. 5 (top) shows a general agreement between observed and simulated values, with higher rates corresponding to periods of relatively high wind speeds and low relative humidity (Fig. 5, bottom). Overall, the cumulative amounts of observed and simulated sublimation were similar, equal to approximately 24 and 26 kg m^{-2} over the period, respectively.

4.3 Simulation of energy fluxes to snow

To investigate CRHM's handling of energy fluxes, simulations of energy fluxes to snow were compared to measurements made at the Marmot Creek paired pine forest and clearing sites. Measurements from these sites include incoming and outgoing shortwave and longwave radiation, as well as ground heat fluxes. However, as no direct measures of sensible and latent heat were made, evaluation of the simulation of these fluxes was not possible.

Time-series plots of observed and simulated energy terms during snowcover in Fig. 6 and model indices in Table 5 show a good agreement for all shortwave radiation terms at forest and clearing sites, and good prediction of net longwave radiation (L^*) at the clearing site. However, even with the good prediction of the individual incoming and outgoing longwave fluxes ($L\downarrow$ and $L\uparrow$) at the forest, the prediction of forest L^* was poor, which contributed to degrading estimates of total net radiation to forest snow (i.e. $Q_n = K^* + L^*$). Despite the large errors in estimating the ground energy flux (Q_g) at the forest and clearing sites, little effect on overall model performance resulted due to the small contribution of Q_g to total energy (note that no energy to snow from rainfall, Q_p, was observed or simulated). In terms of systematic bias, the small negative and positive values of L^*, Q_n and Q_g observed (and simulated) provided MB values that were often misleading and not instructive to model assessment. Alternatively, the systematic model bias of energy terms was evaluated simply as the difference between the mean of simulated and observed values. Here, the offsetting of small negative and positive biases of individual energy terms resulted in low bias errors of total energy to snow (Q^*) at the forest and clearing sites of −0.59 and −0.37 W m^{-2}, respectively. Furthermore, the close comparison of total simulated and observed energy terms in Fig. 7 demonstrate that CRHM was

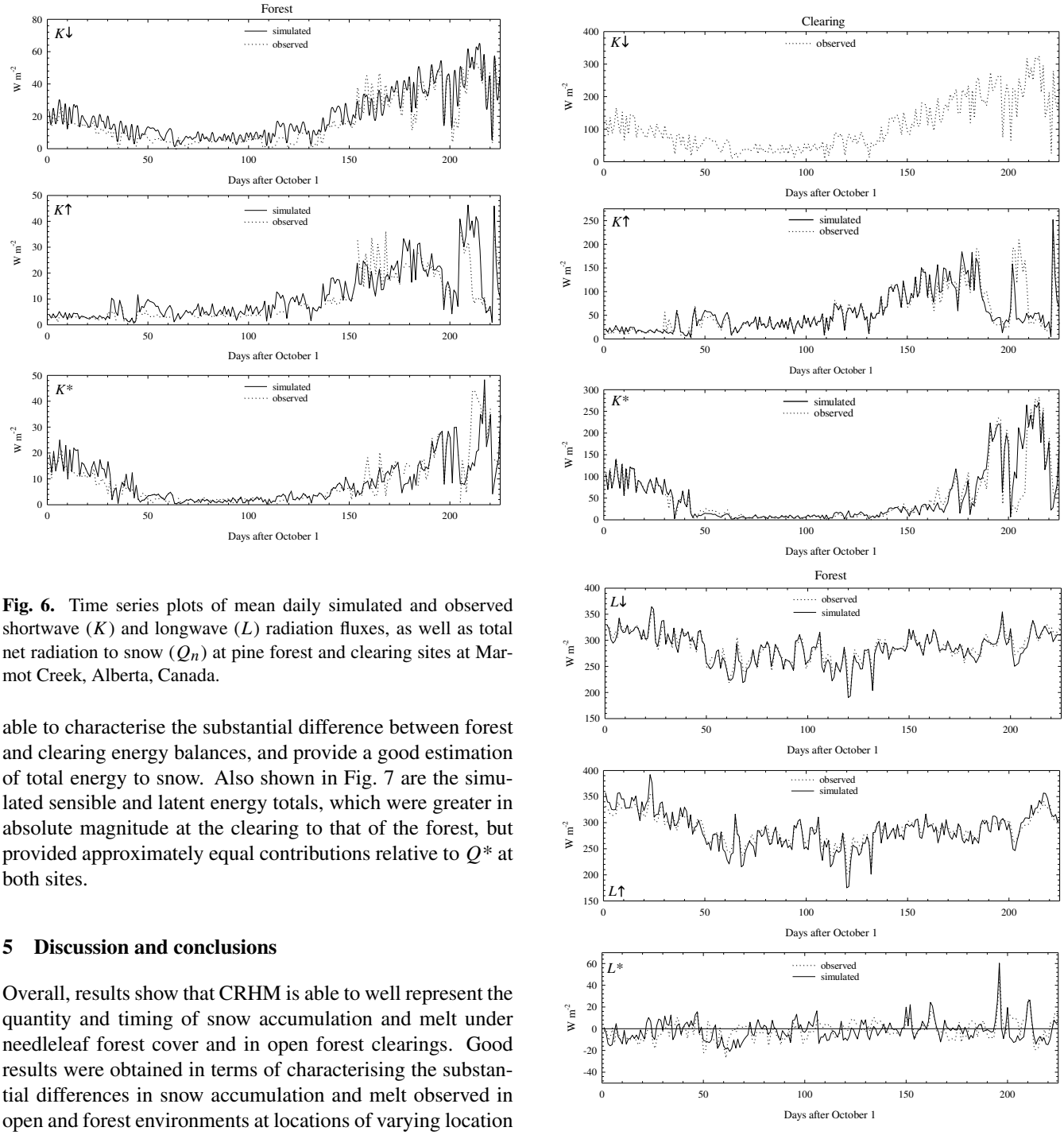

Fig. 6. Time series plots of mean daily simulated and observed shortwave (K) and longwave (L) radiation fluxes, as well as total net radiation to snow (Q_n) at pine forest and clearing sites at Marmot Creek, Alberta, Canada.

able to characterise the substantial difference between forest and clearing energy balances, and provide a good estimation of total energy to snow. Also shown in Fig. 7 are the simulated sensible and latent energy totals, which were greater in absolute magnitude at the clearing to that of the forest, but provided approximately equal contributions relative to Q^* at both sites.

5 Discussion and conclusions

Overall, results show that CRHM is able to well represent the quantity and timing of snow accumulation and melt under needleleaf forest cover and in open forest clearings. Good results were obtained in terms of characterising the substantial differences in snow accumulation and melt observed in open and forest environments at locations of varying location and climate. The accurate representation of the major energy terms between the pine forest and clearing sites suggests that despite modest data requirements, the physical basis of the model is sufficient for representing forest-snow processes in environments of varying forest cover and meteorology.

Simulations of mean and maximum seasonal SWE exhibited little systematic bias at forest sites, clearing sites, or all sites. This suggests that much of the errors incurred were random in nature, resulting either from errors in observations or model parameterisation. For simulations of SWE at indi-

Fig. 6. Continued.

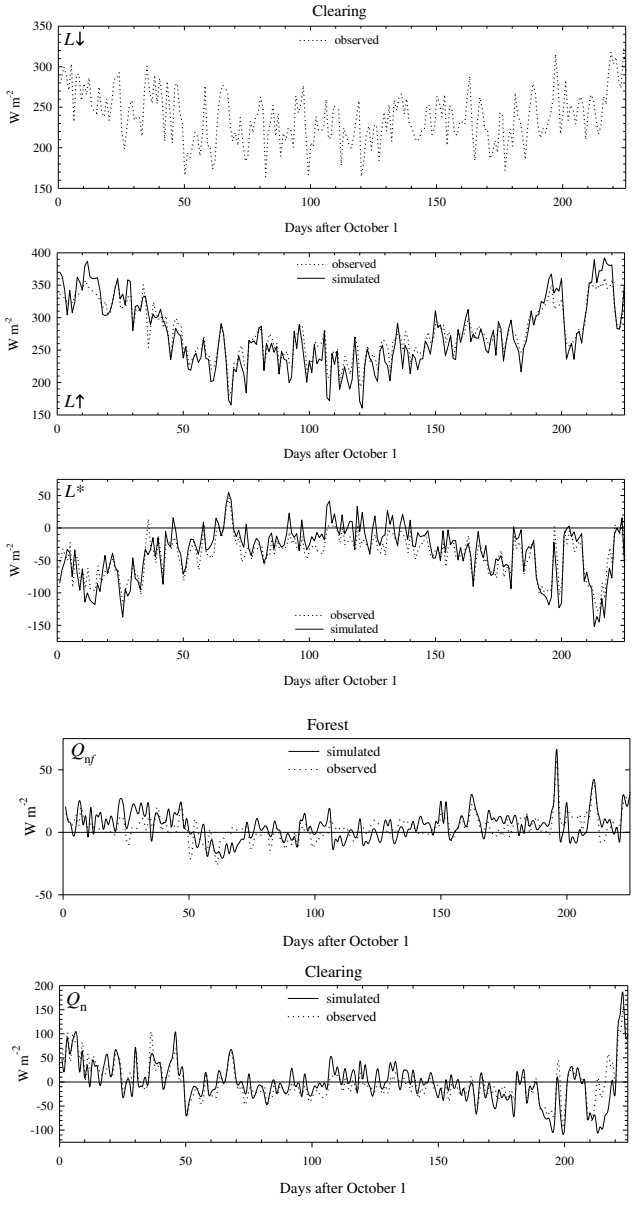

Fig. 6. Continued.

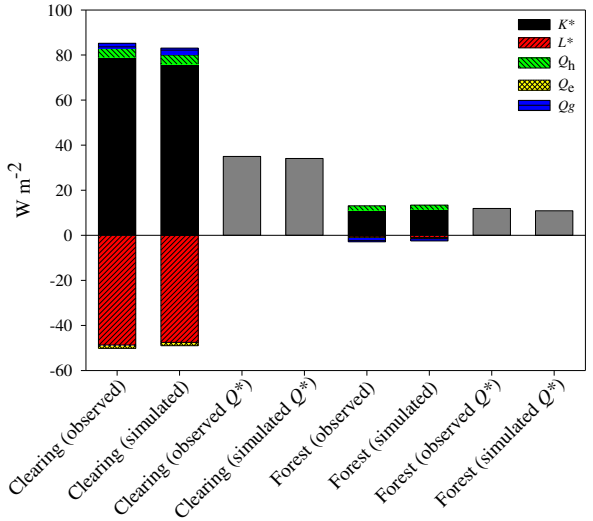

Fig. 7. Observed and simulated net energy terms and total energy to snow ($Q^* = \mathrm{d}U/\mathrm{d}t + Q_m$) at pine forest and clearing sites (note that due to no observations of simulated sensible (Q_h) and latent (Q_e) heat fluxes, observations are assigned the same value as simulations).

vidual sites, errors also appear to be random rather than systematic, considering that the best and worst model efficiencies were obtained for the same site over consecutive winters (i.e. Alptal forest). In all, the poorest model efficiencies of SWE determinations were realised at the 2003–2004 Alptal forest and Marmot pine sites, which had substantially lower accumulations relative to most other sites. Such results may be expected as shallower snowpacks would be more sensitive to simulation errors of mass and energy, thus giving larger relative errors. Notwithstanding these limitations, encouraging simulation results were obtained, as exemplified in the good representation of the extreme differences in forest and clearing snow accumulations observed over the two winters at the Alptal location.

Although good prediction of SWE was made for the start and peak of winter accumulations, poorer predictions were made at the end of accumulation, suggesting a lag in simulated melt rates. Particularly large lags in simulated snow depletion occured at the Alptal (2003–2004) clearing and Marmot spruce clearing sites, where the substantial late-season snowfall may have resulted in an overestimation of the additional energy deficit to the snowpack. As such, improvement in CRHM's representation of snowmelt timing and rate may require addressing the handling of internal snow energetics with large snowfalls.

Compared to observations of canopy snow load changes from a suspended tree, satisfactory model simulation of canopy sublimation was achieved both in terms of daily and cumulative losses. The correspondence of periods of high sublimation with relatively high wind speeds and low relative humidity demonstrate the physically-based manner in which canopy sublimation is accounted for by CRHM. Accordingly, such approaches are likely necessary to predict differences in snow accumulation between forest and clearings resulting from variations in forest cover density and climate. However, sensitivity analysis has shown sublimation estimates in CRHM to be very responsive to errors in the intercepted snowload, which may have been brought about by the rather simplistic approach in the handling of canopy snow unloading by CRHM. Consequently, increased confidence in the model's representation of canopy sublimation losses would likely by gained through a better understanding of the physical processes controlling canopy unloading of snow.

Table 5. Model efficiency index (ME), root mean square error (RMSE), and the difference between mean simulated and observed values of: shortwave irradiance ($K\downarrow$), reflected shortwave irradiance ($K\uparrow$), net shortwave radiation ($K*$), longwave irradiance ($L\downarrow$), longwave exitance ($L\uparrow$), net longwave radiation ($L*$), total net radiation (Q_n), net ground heat flux (Q_g), and total energy to snow ($Q*$) (i.e. $Q^* = Q_m + \mathrm{d}U/\mathrm{d}t$) for pine forest and clearing sites at Marmot Creek, Alberta, Canada.

Site:	$K\downarrow$	$K\uparrow$	$K*$	$L\downarrow$	$L\uparrow$	$L*$	Q_n	Q_g	[a] $Q*$
ME (Clearing) []	–	0.94	0.94	–	0.82	0.67	0.80	−0.92	0.78
ME (Forest) []	0.87	0.82	0.83	0.90	0.79	0.08	0.27	−2.77	0.25
RMSE (Clearing) [W m^{-2}]	–	13.9	13.9	-	18.2	18.2	22.4	1.8	23.1
RMSE (Forest) [W m^{-2}]	6.1	5.3	2.7	9.24	13.1	8.56	9.08	2.2	9.64
Mean simulated – mean observed (Clearing) [W m^{-2}]	–	2.75	−2.75	–	−3.15	3.15	0.40	−0.03	−0.37
Mean simulated – mean observed (Forest) [W m^{-2}]	0.36	−0.02	0.38	−2.70	−1.70	−1.0	−0.60	0.02	−0.59

[a] excludes sensible and latent heat fluxes

Although simulations of energy fluxes were evaluated against observations at only a single paired forest and clearing site, results show the model able to well represent both the total energy to snow and the relative contributions of individual energy terms. Furthermore, all errors in estimating shortwave and longwave radiation were small and below the measurement error of the radiometers used in their observation. However, the presence of forest cover is seen to dramatically decrease the model's predictive capability of net radiation and total energy to snow, as seen in the decreasing model efficiency with the increasing number of combined energy terms. Yet, cumulative errors in estimating total energy to snow were relatively modest, owing in part to the error cancellation of individual energy terms. Although no evaluation of sensible and latent energy terms was possible, simulated magnitudes were similar to those observed in cold-region needleleaf forest environments by Harding and Pomeroy (1996) and estimated by Pomeroy and Granger (1997).

Despite some uncertainly in model performance, results show CRHM is able to provide good characterisation of critical forest-snow processes in environments of highly variable forest cover and climate, with only modest requirements for site information and meteorological forcing data. As simulations were performed without calibration to any objective function, there is increased confidence that CRHM is capable of representing the effects on snow accumulation and melt brought about by changes in forest cover or climate. Consequently, results from this model evaluation are encouraging for the use of CRHM as a diagnostic or predictive tool in investigating needleleaf forest cover effects on snow processes in cold regions.

Appendix A

Notation

B	fraction of ice in wet snow []
C	Celsius [°]
C_c	fraction of horizontal canopy coverage []
C_e	intercepted snow exposure coefficient []
C_l	"canopy-leaf contact area" per unit ground []
c_p	specific heat capacity of air [J kg^{-1} K^{-1}]
C_R	canopy rain depth [mm]
E	evaporation from a partially-wetted canopy [kg m^{-2} t^{-1}]
E_p	evaporation from a fully-wetted canopy [kg m^{-2} t^{-1}]
e_a	vapour pressure [kPa]
ea_{mean}	mean daily vapour pressure [kPa]
F	exponent value []
h	forest height [m]
H_{in}	incoming horizontal snow transport rate [kg m^{-2} t^{-1}]
H_{out}	outgoing horizontal snow transport rate [kg m^{-2} t^{-1}]
hr	hour []
I_r	canopy rainfall interception rate [kg m^{-2} t^{-1}]
$I_{r,o}$	canopy intercepted rainload [kg m^{-2}]
I_s	canopy snowfall interception rate [kg m^{-2} t^{-1}]
$I_{s,o}$	canopy intercepted snowload [kg m^{-2}]
I^*_s	species-specific maximum intercepted snowload [kg m^{-2}]
k	intercepted snow shape coefficient []
K	degrees Kelvin []
$K\downarrow$	shortwave irradiance [MJ m^{-2} t^{-1} or W m^{-2}]
$K\downarrow_f$	sub-canopy shortwave irradiance [MJ m^{-2} lt^{-1} or W m^{-2}]
$K\uparrow$	reflected shortwave irradiance [MJ m^{-2} t^{-1} or W m^{-2}]
$K*$	net shortwave radiation [MJ m^{-2} t^{-1} or W m^{-2}]
$L\downarrow$	longwave irradiance [MJ m^{-2} t^{-1} or W m^{-2}]
$L\downarrow_f$	sub-canopy longwave irradiance [MJ m^{-2} t^{-1} or W m^{-2}]
$L\uparrow$	surface longwave exitance [MJ m^{-2} t^{-1} or W m^{-2}]
$L*$	net longwave radiation [MJ m^{-2} t^{-1} or W m^{-2}]
LAI'	effective leaf area index []
M	snowmelt rate [kg m^{-2} t^{-1}]
MB	model bias index []
ME	model efficiency index []
n	number []
P	precipitation rate [kg m^{-2} t^{-1}]
P_r	rainfall rate [kg m^{-2} t^{-1}]
P_s	snowfall rate [kg m^{-2} t^{-1}]
q_e	canopy sublimation rate [kg m^{-2} s^{-1}]
Q_e	net latent heat flux [MJ m^{-2} t^{-1} or W m^{-2}]
Q_g	net ground heat flux [MJ m^{-2} t^{-1} or W m^{-2}]
Q_h	net sensible heat flux [MJ m^{-2} t^{-1} or W m^{-2}]
Q_m	snowmelt energy [MJ m^{-2} t^{-1} or W m^{-2}]
Q_n	total net radiation to snow [MJ m^{-2} t^{-1} or W m^{-2}]
Q_{nf}	total net radiation to forest snow [MJ m^{-2} t^{-1} or W m^{-2}]
Q_p	energy from rainfall advection [MJ m^{-2} t^{-1} or W m^{-2}]
Q^*	net energy to snow [MJ m^{-2} t^{-1} or W m^{-2}]
r_a	aerodynamic resistance [s m^{-1}]
R_d	canopy rain drip rate [kg m^{-2} t^{-1}]
RH	relative humidity [%]
RMSE	root mean square error [units variable]
S	sublimation loss rate [kg m^{-2} t^{-1}]
$\overline{S}$	mean maximum snowload per unit area of branch [kg m^{-2}]
SWE	snow water equivalent [kg m^{-2}]
SWE$_o$	antecedent snow water equivalent [kg m^{-2}]
t	timestep [variable]
T_a	air temperature [°C or K]
T_b	threshold ice-bulb temperature for snow unloading [°C]
T_f	forest temperature [K]
T_{max}	maximum daily air temperature [°C]
T_r	rainfall temperature [°C]
u	wind speed [m s^{-1}]
u_h	wind speed at canopy top [m s^{-1}]
u_{mean}	mean daily wind speed [m s^{-1}]
u_ξ	within-canopy wind speed at depth ξ from canopy top [m s^{-1}]
U	internal (stored) snow energy [MJ m^{-2} t^{-1}]
U_l	canopy snow unloading rate [kg m^{-2} t^{-1}]
V_i	sublimation rate of intercepted snow [s^{-1}]
V_s	simulated sublimation flux for a 500 μm radius ice-sphere [s^{-1}]
x_{avg}	average observed value []
x_{obs}	observed value []
x_{sim}	simulated value []
α_s	snow albedo []
λ_f	latent heat of fusion [MJ kg^{-1}]
λ_s	latent heat of sublimation [MJ kg^{-1}]
Δ	slope of saturation vapour pressure curve [kPa K^{-1}]
ε_f	thermal emissivity of forest cover []
ε_s	thermal emissivity of snow []
θ	solar elevation angle [radians]
ξ	depth from canopy top (as a fraction of forest height) []
ρ_a	density of air [kg m^{-3}]
ρ_s	density of snowfall [kg m^{-3}]
ρ_w	density of water [kg m^{-3}]
σ	Stefan-Boltzmann constant [W m^{-2} K^{-4}]
τ	forest shortwave transmittance []
v	sky view factor []
ψ	canopy wind speed extinction coefficient []
w_a	specific mixing ratio of air []
w_s	saturation mixing ratio of air []

Acknowledgements. The authors would like to thank R. Essery and N. Rutter for their efforts in facilitating the SnoMIP2 initiative, which provided an invaluable opportunity for model evaluation and improvement. Funding and support was provided by the Natural Sciences and Engineering Research Council of Canada Alexander Graham Bell Doctoral and Michael Smith Foreign Student Supplement scholarships and Discovery Grants, the Canada Research Chairs Program, the Canadian Foundation for Climate and Atmospheric Science IP3 Network, Alberta Department of Sustainable Resource Development, the Canada Foundation for Innovation (CFI), the Natural Environment Research Council (UK), the GEWEX Americas Prediction Project (GAPP), and the Biogeosciences Institute, University of Calgary.

Edited by: W. Quinton

References

Anderson, E. A.: A point energy and mass balance model of a snow cover, NWS Technical Report 19, National Oceanic and Atmospheric Administration, Washington, DC, USA, 150 pp., 1976.

Eagleson, P. S.: Ecohydrology, Darwinian expression of vegetation form and function, Cambridge University Press, Cambridge, UK, 443 pp., 2002.

Ellis, C., Pomeroy, J., Essery, R., and Link, T.: Effects of needleleaf forest cover on radiation to snow and snowmelt dynamics in the Canadian Rocky Mountains, Can. J. Forest Res., submitted, 2010.

Essery, R., Rutter, N., Pomeroy, J., Baxter, R., Stähli, R., Gustafsson, D., Barr, A., Bartlett, P, and Elder, K.: An evaluation of forest snow process simulations, B. Am. Meteorol. Soc., 90(8), 1120–1135, 2009.

Essery, R. L. H., Pomeroy, J. W., Ellis, C., and Link, T.: Modelling longwave radiation to snow beneath forest canopies using hemispherical photography and linear regression, Hydrol. Process., 22, 2788–2800, doi:10.1002/hyp.6630, 2008.

Flerchinger, G. N. and Saxton, K. E.: Simultaneous heat and water model of a freezing snow-residue-soil system I. Theory and development, Trans. of ASAE, 32(2), 565–571, 1989.

Gelfan, A., Pomeroy, J. W., and Kuchment, L.: Modelling forest cover influences on snow accumulation, sublimation and melt, J. Hydrometeorol., 5, 785–803, 2004.

Gray, D. M. and Male, D. H. (Eds): Handbook of Snow: Principles, Processes, Management and Use, Pergamon Press, Toronto, Canada, 776 pp., 1981.

Gray, D. M. and Landine, P. G.: An energy budget snowmelt model for the Canadian Prairies, Can. J. Earth Sci., 22(3), 464–472, 1988.

Gryning, S. and Batchvarova, E.: Energy balance of a sparse coniferous high-latitude forest under winter conditions, Boundary Layer Meteorology, 99, 465–488, 2001.

Harding, R. J. and Pomeroy, J. W.: The energy balance of the winter boreal landscape, J. Climate, 9, 2778–2787, 1996.

Hardy, J. P., Melloh, R., Robinson, P., and Jordan, R.: Incorporating effects of forest litter in a snow process model, Hydrol. Process., 14, 3227–3237, 2000.

Hardy, J., Melloh, R., Koenig, G., Marks, D., Winstral, A., Pomeroy, J. and Link, T.: Shortwave radiation transmission through conifer canopies, Agr. Forest. Meteorol., 126, 257–270, 2004.

Hedstrom, N. R. and Pomeroy, J. W.: Measurements and modelling of snow interception in the boreal forest, Hydrol. Process., 12, 1611–1625, 1998.

Hellström, R. Å.: Forest cover algorithms for estimating meteorological forcing in a numerical snow model, Hydrol. Process., Special Issue: Eastern Snow Conference, 14(18), 3239–3256, 2000.

Jordan, R.: Special Report 91–16, A one-dimensional temperature model for a snow cover, Technical documentation for SNTHERM.89. US Army Corps of Engineers Cold Regions Research and Engineering Laboratory, Hanover, New Hampshire, 49 pp., 1991.

Koivusalo, H. and Kokkonen, T.: Snow processes in a forest clearing and in a coniferous forest, J. Hydrol., 262, 145–164, 2002.

Link, T. E. and Marks, D.: Point simulation of seasonal snow cover dynamics beneath boreal forest canopies, J. Geophys. Res., 104, 27841–27857, 1999.

Link, T. E., Marks, D., and Hardy, J.: A deterministic method to characterize canopy radiative transfer properties. Hydrol. Process., 18, 3583–3594, 2004.

Lundberg, A. and Halldin, S.: Evaporation of intercepted snow, analysis of governing factors, Water Resour. Res., 30, 2587–2598, 1994.

Marks, D., Domingo, J., Susong, D., Link, T., and Garen, D.: A spatially distributed energy balance snowmelt model for application in mountain basins, Hydrol. Process., 13, 1935–1959, 1999.

McNay, R. S., Petersen, L. D., and Nyberg, J.B.: The influence of forest stand characteristics on snow interception in the coastal forests of British Columbiam, Can. J. Forest Res., 18, 566–573, 1988.

Melloh, R. A., Hardy, J. P., Bailey, R. N., and Hall, T. J.: An efficient snow albedo model for the open and sub-canopy, Hydrol. Process., 16, 3571–3584, 2002.

Metcalfe, R. A. and Buttle, J. M.: Controls of canopy structure on snowmelt rates in the boreal forest, Proceedings of the 52nd Eastern Snow Conference, 249–257, 1995.

Monteith, J. L.: Evaporation and environment, Sym. Soc. Exp. Biol., 19, 205–234, 1965.

Parviainen, J. and Pomeroy, J. W.: Multiple-scale modelling of forest snow sublimation, initial findings, Hydrol. Process., 14, 2669–2681, 2000.

Pomeroy, J. W. and Schmidt, R. A.: The Use of Fractal Geometry in Modelling Intercepted Snow Accumulation and Sublimation, Proceedings of the Eastern Snow Conference, 50, 1–10, 1993.

Pomeroy, J. W. and Gray, D. M.: Snowcover Accumulation, Relocation and Management, NHRI Science Report No. 7, National Hydrology Research Institute, Environment Canada, Saskatoon, SK, 134 pp., 1995.

Pomeroy., J. W. and Dion, K.: Winter radiation extinction and reflection in a boreal pine canopy, measurements and modelling, Hydrol. Process., 10, 1591–1608, 1996.

Pomeroy, J. W. and Granger, R. J.: Sustainability of the western Canadian boreal forest under changing hydrological conditions – I-snow accumulation and ablation, in: :Sustainability of Water Resources under Increasing Uncertainty, edited by: Rosjberg, D., Boutayeb, N., Gustard, A., Kundzewicz, Z., and Rasmussen, P., IAHS Publ No. 240, IAHS Press, Wallingford, UK, 237–242,

1997.

Pomeroy, J. W., Parviainen, J., Hedstrom, N., and Gray, D. M.: Coupled modelling of forest snow interception and sublimation, Hydrol. Process., 12, 2317–2337, 1998a.

Pomeroy, J. W., Gray, D. M., Hedstrom, N. R., and Janowicz, J. R.: Prediction of seasonal snow accumulation in cold climate forests, Hydrol. Process., 16, 3543–3558, 2002.

Pomeroy, J. W., Gray, D. M., Brown, T., Hedstrom, N. R., Quinton, W. L., Granger, R. J., and Carey, S. K.: The cold regions hydrological model, a platform for basing process representation and model structure on physical evidence, Hydrol. Process., 21(20), 2650–2667, 2007.

Pomeroy, J. W., Marks, D., Link, T., Ellis, C., Hardy, J., Rowlands, A., and Granger, R.: The impact of coniferous forest temperature on incoming longwave radiation to melting snow, Hydrol. Process., 23(17), 2513–2525, doi:10.1002/hyp.7325, 2009.

Rutter, N., Essery, R., Pomeroy, J., Altimir, N., Andreadis, K., Baker, I., Barr, A., Bartlett, P., Boone, A., Deng, H., Douville, H., Dutra, E., Elder, K., Ellis, C., Feng, X., Gelfan, A., Goodbody, A., Gusev, Y., Gustafsson, D., Hellstrom, R., Hirabayashi, Y., Hirota, T., Jonas, T., Koren, V., Kuragina, A., Lettenmaier, D., Li, W-P, Martin, E., Nasanova, O., Pumpanen, J., Pyles, R., Samuelsson, P., Sandells, M., Schadler, G., Shmakin, A., Smirnova, T., Stahli, M., Stockli, R., Strasser, U., Su, H., Suzuki, K., Takata, K., Tanaka, K., Thompson, E., Vesala, T., Viterbo, P., Wiltshire, A., Xia, K., Xue, Y., and Yamazaki, T.: Evaluation of forest snow process models (SnowMip2), J. Geophys. Res.-Atmos., 114, D06111, doi:10.1029/2008JD011063, 2009.

Rutter, A. J., Kershaw, K. A., Robins, P. C., Morton, A. J.: A predictive model of rainfall interception in forests. I. Derivation of the model from observations in a plantation of Corsian pine, Agr. Meteorol., 9, 367–384, 1971.

Schmidt, R. A., Jairell, R. L., and Pomeroy, J. W.: Measuring snow interception and loss from an artificial conifer, P. West. Snow Conf., 56, 166–169, 1988.

Schmidt, R. A.: Sublimation of snow by an artificial conifer, Agr. Forest Meteorol., 54, 1–27, 1991.

Sicart, J. E., Pomeroy, J. W., Essery, R. L. H., Hardy, J. E., Link, T., and Marks, D.: A sensitivity study of daytime net radiation during snowmelt to forest canopy and atmospheric conditions, J. Hydrometeorol., 5, 744–784, 2004.

Troendle, C. A. and King, R. M.: The effect of timber harvest on the Fool Creek watershed: 30 years later, Water Resour. Res., 21, 1915–1922, 1985.

Valente, F., David, J. S. and Gash, J. H. C.: Modelling interception loss for two sparse eucalypt and pine forests in central Portugal using reformulated Rutter and Gash analytical models, J. Hydrol., 190, 141–162, 1997.